JOURNAL OF GEOPHYSICAL RESEARCH, VOL. 101, NO. B11, PAGES 25,403–25,421, NOVEMBER 10, 1996

Postrifting anelastic deformation around the spreading plate boundary, north Iceland 1. Modeling of the 1987–1992 deformation field using a viscoelastic Earth structure

M. A. Hofton
Institute of Geophysics and Planetary Physics, Scripps Institution of Oceanography
La Jolla, California

G. R. Foulger
Department of Geological Sciences, University of Durham, Durham, England

Abstract.
A third Global Positioning System (GPS) survey of a regional network surrounding the Krafla volcanic system, north Iceland, was conducted in 1992 following a major crustal spreading episode which began in this system in 1975. Differencing the 1992 results with those from 1987 and 1990 reveals a regional deformation field with a maximum, rift-normal expansion rate of 4.5 cm/year near the rift, decreasing to 3 cm/year at large distances. The time-averaged spreading rate in north Iceland, 1.8 cm/year, cannot account for this deformation. The vertical deformation field reveals regional uplift throughout the network area at its maximum closest to the rift and decreasing with distance. Three different models are applied to study the postdike injection ground deformation: (1) stress redistribution in an elastic layer over a viscoelastic half-space, (2) stress redistribution in an elastic-viscous layered medium, and (3) continued opening at depth on the dike plane in an elastic half-space. Using model 1, the effects of historical episodes in the region are subtracted from the observed displacement fields, and the remaining motion is modeled as relaxation following the recent Krafla rifting episode. The best fit model involves a half-space viscosity of 1.1 x 10^{18} Pa s, a relaxation time of 1.7 years, and an elastic layer thickness for northeast Iceland of 10 km. The vertical field indicates that the Krafla dike complex rifted the entire elastic layer. Using model 2, the motion 1987–1990 and 1990–1992 can be simulated adequately given the survey errors, but the 1987–1992 deformation is poorly fitted, suggesting that a more realistic geophysical model is required. Using model 3, a range of dikes will fit the deformation field.

Introduction

The Krafla volcanic system, which contains a 100 km-long, NNE-striking fissure swarm and a central volcano, is one of five en échelon volcanic systems that together constitute the Northern Volcanic Zone (NVZ) of Iceland (Figure 1), where plate growth is taking place. A major rifting episode lasting about a decade began in the Krafla volcanic system in December 1975 [*Björnsson et al.*, 1977, 1979], involving about 20 rifting events. During each event, magma flowed rapidly out of a crustal magma chamber underlying the Krafla central volcano into the fissure swarm forming dikes and, in nine instances, resulted in volcanic eruptions. This activity was accompanied by migrating seismicity and ground movements. The repeated, sudden extension of the fissure swarm caused extensive faulting and fissuring above the intruded dikes and resulted in subsidence of the central part of the fissure swarm and uplift of the flanks. Total widening across the fissure swarm was approximately 2 m along 50 km of its length and 6 m along another 30 km [*Björnsson*, 1985]. The local maximum amount of widening was 9 m [*Gudmundsson*, 1995b].

Major geodetic surveys using the Global Positioning System (GPS) were carried out in 1987 and 1990, ~2 to 5 years after the rifting episode was over. Differencing the results of these surveys revealed large, systematic, rift-normal expansion [*Foulger et al.*, 1992; *Heki et al.*, 1993; *Jahn et al.*, 1994]. These movements were interpreted as postrifting relaxation of compressional

Paper number 96JB02466.
0148-0227/96/96JB-02466$09.00

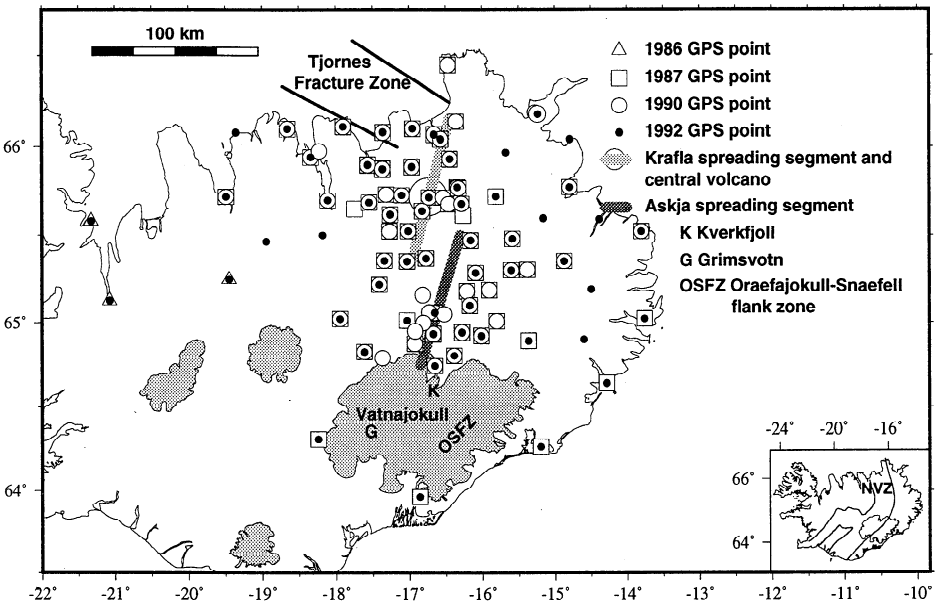

Figure 1. Map of Iceland showing the 1986, 1987, 1990 and 1992 Iceland GPS points. Two of the five en échelon volcanic systems of the neovolcanic zone, the Krafla and Askja volcanic systems, are shown schematically. Inset shows the neovolcanic zone in Iceland. NVZ: Northern Volcanic Zone.

stress accumulated in the near-boundary region of the plates during the recent Krafla rifting episode [*Foulger et al.*, 1992; *Heki et al.*, 1993]. A simple model was used consisting of a thin, elastic plate overlying a thin, Newtonian viscous layer [*Elsasser*, 1969; *Bott and Dean*, 1973]. The 1975–1984 series of dike intrusions was modeled both as a single, instantaneous, infinitely long dike (the one-dimensional model) [*Foulger et al.*, 1992] and as a series of such dikes with finite lengths (the two-dimensional model) [*Heki et al.*, 1993]. The simple Earth model used provided an initial approximation of the process at work, and in this paper the deformation is modeled using a more realistic elastic-viscoelastic Earth model.

GPS Measurements in North Iceland

The Surveys

In July 1987 a network of ~63 ground control points covering an area of ~250 x 250 km was constructed from preexisting and new points and measured using GPS [*Foulger*, 1987; *Jahn et al.*, 1990; *Heki et al.*, 1993] (Figure 1). This and all subsequent fieldwork was collaborative between the Universities of Durham, England, and Hannover, Germany, with contributions also from the Icelandic GPS Coordinating Committee. Points were densely spaced within the Krafla volcanic system and sparsely distributed throughout an area extending 130 km into the adjoining plates. In August 1990 most of the 1987 network was remeasured [*Jahn et al.*, 1990; *Heki et al.*, 1993]. Differencing the results of these surveys revealed up to 18 cm of rift-normal widening for the period 1987–1990 [*Foulger et al.*, 1992; *Heki et al.*, 1993]. The deformation gradient was greatest across the center of the fissure swarm where dike emplacement took place during the Krafla rifting episode. The maximum east-west expansion occurred between points 20–30 km on either side of the rift axis, was approximately 3 times the time-averaged spreading rate for Iceland (1.8 cm/year [*DeMets et al.*, 1994]), and decreased slightly beyond this. Calculated vertical movements were around a few centimeters but were less systematic than the calculated horizontal displacements, which is to be expected as the errors in the vertical component are several times greater than those in the horizontal. However, there was weak evidence that points

Table 1. Repeatabilities and Scaled Formal Errors [*Heki*, 1992] of Site Coordinates at the 1σ Confidence Level in Three Components for the Iceland GPS Surveys

Survey	North-South, mm	East-West, mm	Up-Down, mm
	Repeatability		
1987	6.4	9.2	16.7
1990	10.1	11.0	19.3
1992	7.1	6.2	19.0
	Scaled Formal Errors		
1987	7.8	10.9	17.0
1990	18.9	20.1	30.1
1992	11.1	8.7	24.4

The 1987 and 1990 results are adapted from *Heki et al.* [1993].

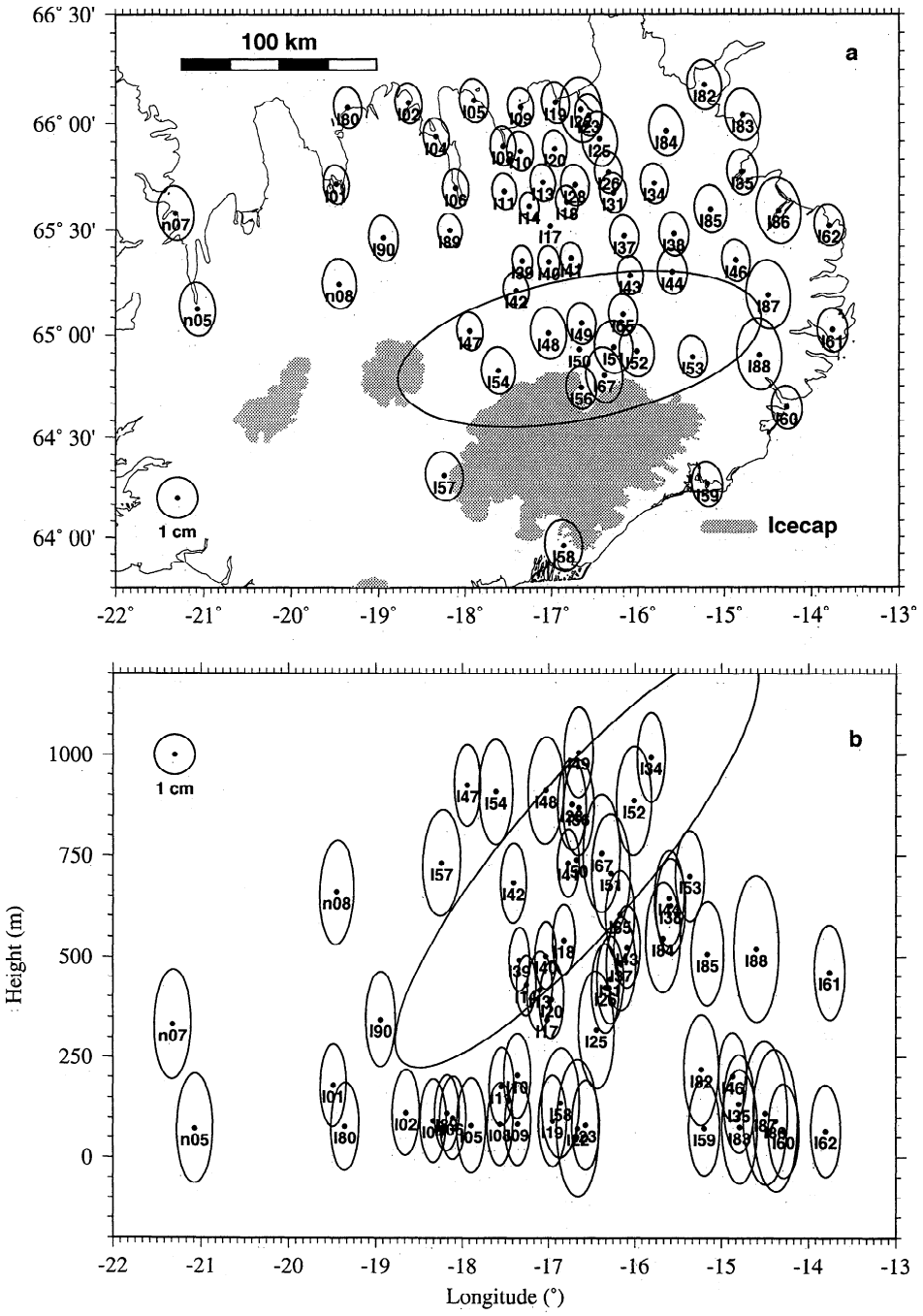

Figure 2. Scaled formal error ellipses at the 68% confidence level for the ambiguity-fixed 1992 network solution, (a) horizontal plane, and (b) longitude versus height. The large scaled formal error associated with point I50 is a result of the very short (~1 hour), single occupation of this point.

in the region of dike emplacement had uplifted relative to those farther south [*Heki et al.*, 1993].

In July/August 1992 much of the existing network was remeasured, along with additional points (Figure 1). The 1992 network was designed on the basis of forward modeling of the 1987–1990 deformation field using the stress diffusion model [*Foulger et al.*, 1992; *Heki et al.*, 1993]. Some closely spaced, redundant points within the neovolcanic zone were omitted and 12 more distant points were added where modeling of the 1987–1990 deformation field predicted substantial motion. Three of these had been occupied using GPS in 1986 [*Foulger et al.*, 1993], and nine were new GPS points to the east, west, and southeast of the network (Figure 1). A total of 62 points were measured over a 20-day period.

Analysis of the Iceland 1992 Data

The data were analyzed using the Bernese version 3.2 software [*Rothacher et al.*, 1990]. The data set is of high quality. Few processing problems were encountered, and ambiguity-fixed solutions were obtained for all the sessions. A network solution, combining the individual

Table 2. Results of the Helmert Transformation Applied to Compare the 1992 Bernese and GEONAP Final Coordinates

Parameter			Result		
Translation, m	x	=	2.50	±	0.003
	y	=	5.70	±	0.003
	z	=	-0.40	±	0.003
Rotation, arc sec	x	=	0.02	±	0.010
	y	=	0.02	±	0.010
	z	=	0.00	±	0.010
Scale factor, mm/km			0.01	±	0.040

The x, y and z are axes in the local (east, north, up) coordinate system.

session coordinate results, was created using the program NETADJ [*Heki*, 1992]. The repeatabilities of the site coordinates were evaluated as the weighted RMS scatter of the differences between the coordinates from the individual sessions and the network solution. The repeatabilities of the north-south and east-west components are of comparable quality and at the subcentimeter level. The repeatability of the up-down component is 3–4 times poorer and is at the 2 cm level (Table 1). Typical scaled formal errors [*Heki*, 1992] of ~1 cm were obtained in the horizontal and ~2 cm in the vertical components (Table 1 and Figure 2). The repeatabilities and scaled formal errors of the 1992 survey are of comparable quality to those of the 1987 survey and are smaller than those from 1990 (Table 1) [*Heki et al.*, 1993]. Thus the 1992 results are of a comparable quality to those from 1987 and of substantially higher quality than those from 1990.

The data were analyzed independently at the University of Hannover using the GEONAP processing software [*Wübbena*, 1989]. The quality of the results can thus be tested further by comparing the final coordinates calculated by the two software packages, the Bernese v3.2 software and the GEONAP software. This was done using a seven-parameter Helmert transformation, consisting of three rotations, three translations, and a scale factor (Table 2). Significant translations were required, a trivial difference resulting from variations in the coordinates of the fixed sites used. No nontranslational parameters are significant at greater

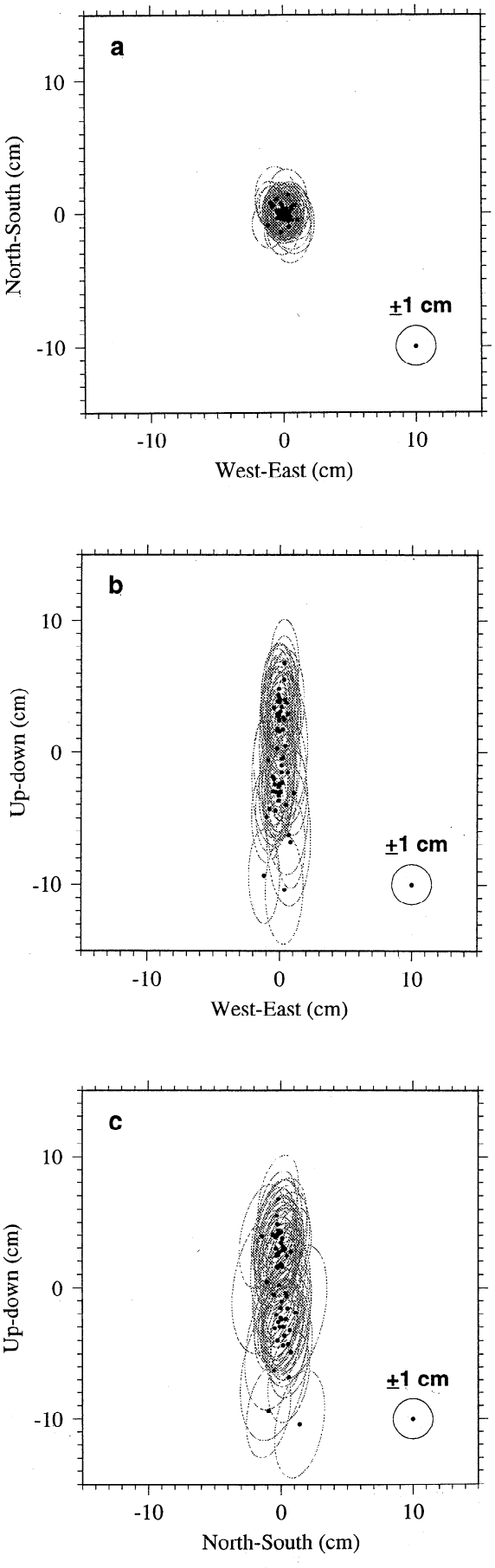

Figure 3. Comparison of the final coordinates of the 1992 survey obtained using the Bernese and GEONAP software packages. The solid dots represent the residuals after a seven-parameter Helmert transformation (Table 2) applied to the Bernese positions with respect to the GEONAP positions. The error ellipses are the Bernese scaled formal errors at the 68% confidence level: (a) north-south versus west-east, (b) up-down versus west-east, and (c) up-down versus north-south.

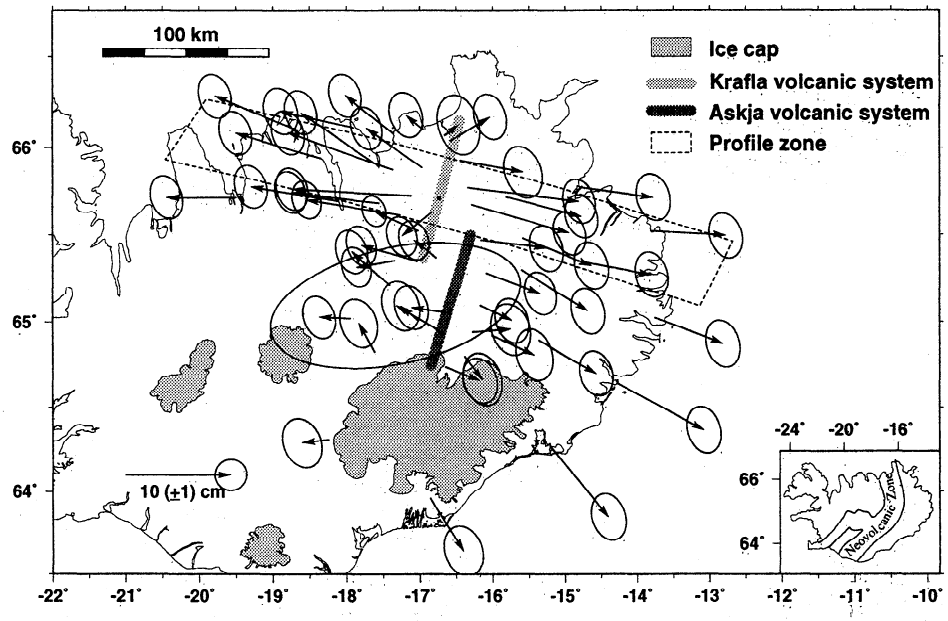

Figure 4. Displacements of GPS points 1987–1992. Ellipses at each arrowhead indicate scaled formal errors at the 68% confidence level. The arrow at lower left gives the scale. The zone of points used to construct the profile shown in Figure 5 is enclosed in a box.

than the 2σ level. Agreement in the point coordinates was within 2 cm in the horizontal components (Figure 3) but much larger, up to 11 cm, in the vertical. This agreement is within 2σ of the scaled formal errors of the Bernese results for the horizontal components, but up to $\sim 6\sigma$ for the vertical. Agreement is worse in the vertical as a result of satellites being visible in one hemisphere only and also because of the different tropospheric models used in the independent data analyses.

Deformation Results

Comparison of the 1987 and 1992 horizontal results indicates a large systematic expansion perpendicular to the plate boundary (Figure 4), which is consistent with continuation of the motion detected by *Foulger et al.* [1992], *Heki et al.* [1993], and *Jahn et al.* [1994] for the 1987–1990 epoch. The 1987–1992 expansion is as much as 22 cm (~4.4 cm/year) within a few tens of kilometers of the rift, decreasing to approximately 15 cm (~3 cm/year) farthest from the central axis. There is a clear radial component to the deformation pattern. The maximum expansion occurs at distances of ±20 km from the rift zone (Figure 5).

The first-order features of the 1987–1992 horizontal displacement field are well-illustrated by the profile shown in Figure 5. The deformation field is fairly sym-

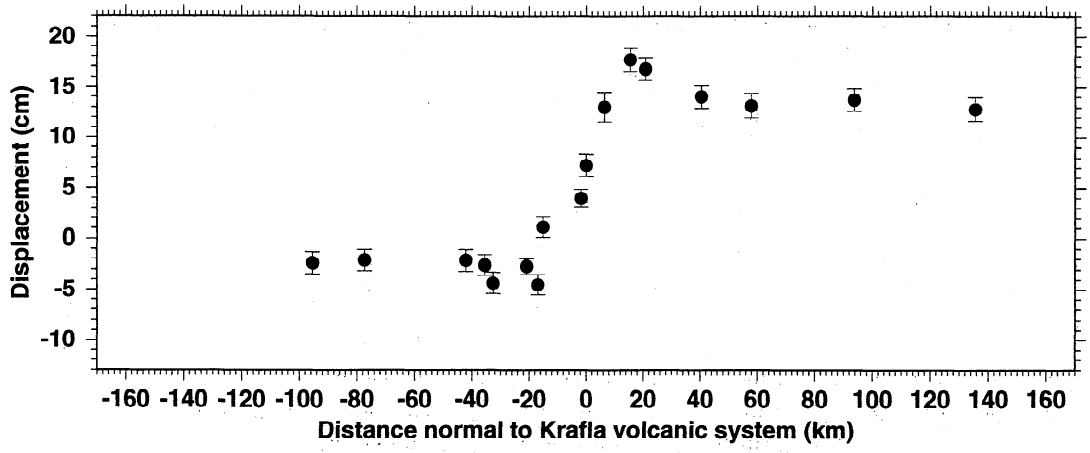

Figure 5. Displacements of GPS points 1987–1992 within the profile zone shown in Figure 4, perpendicular to the Krafla volcanic system, as a function of distance from it. The average trend of the Krafla volcanic system is assumed to be N15°E. The vertical bars indicate 1σ scaled formal errors. Positive displacement occurs to the east of the spreading segment and negative displacement to the west. The zero reference point for displacements is arbitrary.

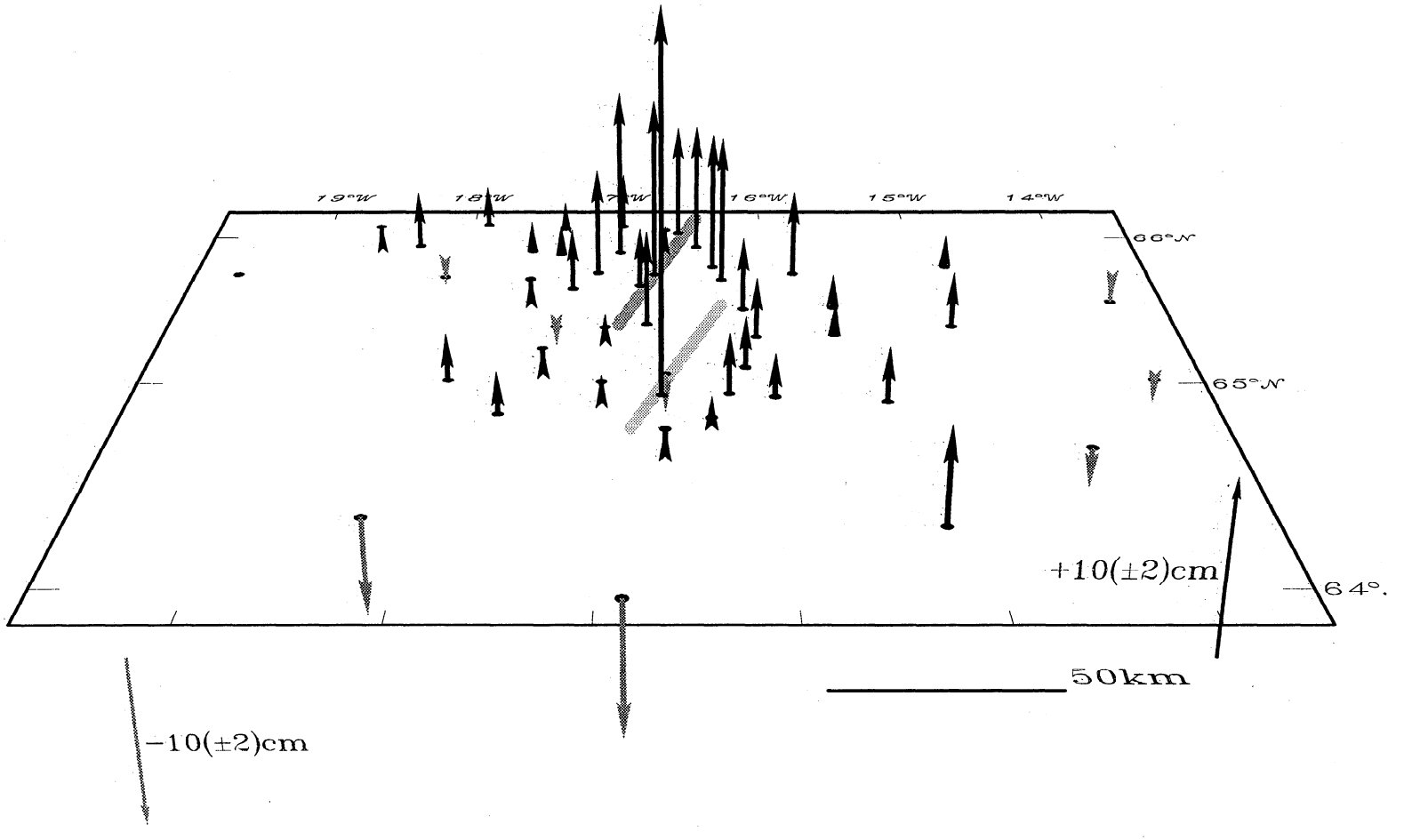

Figure 6. Vertical point displacements for 1987–1992. The two arrows at the base of the figure give the scale of the arrows. All velocities are shown relative to the westernmost point of the network, denoted by a solid oval. The Krafla and Askja volcanic systems are represented by the parallel, dark and light gray shaded lines, respectively. The large, apparent uplift of a single, central point is probably error due to the short, single occupation of this point.

metrical about the Krafla volcanic system. The rate of motion is variable, with high velocities close to the rift which decrease by about 30% farther away. The expansion rate appears to have decreased with time between 1987 and 1992. From 1987 to 1990 the maximum expansion rate was 6.0 ± 0.5 cm/year [*Foulger et al.*, 1994]. This has decreased to 4.5 ± 0.3 cm/year for the period 1987 to 1992. The time-averaged plate motion in northeast Iceland, 1.8 cm/year [*DeMets et al.*, 1994], cannot account for this expansion rate, nor can kinematic models account for the variation in rate.

The vertical displacement field (Figure 6) is shown relative to the westernmost point in the network. Within the Krafla region, points near the rift axis uplift relative to more distant points, with the maximum uplift occurring closest to the rift zone and decreasing with distance.

Deformation Modeling

Introduction

We model the deformation field observed 1987–1992 in Iceland as postrifting stress relaxation in viscoelastic structural elements. Most of the motion is attributable to the 1975–1985 Krafla rifting episode, but we also incorporate the effects of previous rifting episodes, recent large earthquakes, and magma chamber activity.

Following the method of *Rundle* [1978, 1980] and *Hofton et al.* [1995], a model is constructed for a finite, two-dimensional, rectangular dike in an elastic-gravitational layer overlying a viscoelastic-gravitational half-space. The mathematical method used to obtain the near-field, time-dependent displacements, proceeds as follows: (1) The Green's functions for a dilational point source in an elastic layer over an elastic half-space are computed, (2) the correspondence principle [*Lee*, 1955] is applied to introduce viscoelastic properties into the half-space, and (3) the resultant Green's functions are integrated over the finite source region. A linear Maxwell rheology is used for the viscoelastic region. Only gravitational effects dependent on the vertical component of the surface gravitational acceleration g are included in the calculations since *Rundle* [1981] showed that most of the gravitational effects for dislocations arise from the terms associated with g, not with G_0, the gravitational constant.

The computer program, developed to calculate the surface displacements due to dike emplacement and adapted from an existing code to compute surface displacements resulting from a dip-slip source in an elastic-gravitational layer overlying a viscoelastic-gravitational half-space (J. Rundle, personal communication, 1992), was exhaustively tested. In particular, it was tested against the uniform half-space model of *Okada* [1985] and shows a good fit. The predicted surface displacements from a dike in both an extremely thick and extremely thin elastic layer over a viscoelastic half-space were compared with the predictions of *Okada* [1985] and were in reasonable agreement. Possible errors associated with the time-dependent relaxation process were sought by calculating the surface deformation for a dike in an elastic layer over a fully relaxed half-space. Reasonable results, similar to the expected step function response, were obtained. We are therefore confident of the correct working of the program.

A forward modeling approach was taken to determine the model parameters and the best fit model selected from a suite of results. In order to reduce the number of variables, certain model parameters for which strong, independent constraints exist were assumed known, and their values were held fixed during the modeling process. These are the elastic moduli of the elastic layer, μ_l and λ_l, and the half-space, μ_h and λ_h, and the densities of the layer and the half-space, ρ_l, and ρ_h. Seismic refraction experiments suggest an average value for v_p of 5.5 km/s at 0–10 km depths and 7.0–7.4 km/s at 10–30 km depths [*Gebrande et al.*, 1980]. The v_p/v_s ratio for the crust is about 1.76, and 1.96–2.2 for the upper mantle [*Gebrande et al.*, 1980]. Using the standard seismological relations $\mu = v_s^2\rho$ and $\lambda = v_p^2\rho - 4/3\mu$, and a velocity–density relationship of $\rho = 1530 + 230v_p$ [*Christensen and Wilkins*, 1982], values for the densities and elastic moduli of the layer and half-space were calculated (Table 3).

The values of the elastic layer thickness H, the dike heights W, and the dike dips ψ, were constrained within limits by independent results and refined by the modeling described here. A value of 10 km for the elastic layer thickness was consistent with the deformation observations. This is the approximate depth to the regional, low-resistivity layer beneath north Iceland in the neighborhood of the Krafla system, inferred from magnetotelluric evidence [*Björnsson*, 1985] and is further supported by the observed depth extent of earthquakes [*Einarsson*, 1991]. Dikes that ruptured most of the elastic layer, i.e., were ~10 km high, were required to model the deformation field. Such heights are considerably greater than those predicted from the volume of magma flowing out of the magma chamber. However,

Table 3. Parameters Used to Model the 1987–1992 Deformation Field

Model Parameter	Symbol	Value
Elastic layer thickness	H	10 km
Dike height	W	10 km
Dip	ψ	90°
Elastic moduli	μ_l	2.7 x 10^{10} Pa
Layer	λ_l	4.9 x 10^{10} Pa
Half-space	μ_h	4.1 x 10^{10} Pa
	λ_h	9.9 x 10^{10} Pa
Layer density	ρ_l	2800 kg/cm^3
Half-space density	ρ_h	3100 kg/cm^3
Viscosity	η	1.1 x 10^{18} Pa s

they are in accordance with the models of *Björnsson* [1985] and *Gudmundsson* [1995a], whereby magma rising from below during rifting makes up the lower part of the dike complex, and the results of *Rubin* [1992], who calculated the depth to the base of the intruded dikes to be as deep as 8.5 km by inverse modeling of leveling data collected 1975–1980. If periodic rifting episodes rupture the entire elastic layer, then far-field, plate-like motion may be modeled as the summed effect of all large rifting episodes and earthquakes along the plate boundary: the inclusion of uniform "plate motion" outside a "plate boundary zone" is not required. Vertical model dikes are in agreement with the deformation field and are also concordant with field geological observations [*Gudmundsson*, 1995a].

Very few independent estimates of the viscosity of the material beneath Iceland exist, and none exist for timescales of the order of a decade. Estimates of 1–50 x 10^{18} Pa s were obtained from isostatic rebound [*Sigmundsson*, 1991; *Sigmundsson and Einarsson*, 1992] and of 0.3–20 x 10^{18} Pa s by early modeling of the deformation field in north Iceland [*Foulger et al.*, 1992; *Heki et al.*, 1993]. A wide range of possible viscosities were thus tried in the modeling process. A value of 1.1 x 10^{18} Pa s for the viscosity of the half-space was found to be most consistent with the 1987–1992 deformation field, which implies a relaxation time of 1.7 years.

Historical Episodes and Earthquakes

Crustal extension by rifting is thought to occur at about 150-year intervals in the NVZ [*Björnsson et al.*, 1977]. In addition, large earthquakes occur in the Tjörnes Fracture Zone (TFZ) (Figure 1), most recently in 1976, and a magma chamber beneath the Askja volcano is thought to have deflated 1987–1992 (Figure 7). These processes resulted in significant surface deformation from 1987 to 1992.

Rifting is known to have occurred in the Askja volcanic system 1874–1876, in the Krafla volcanic system 1724–1729 (the Mývatn fires episode), and in the Theistareykir volcanic system 1618 [*Björnsson et al.*, 1977] (Figure 7). Dike thicknesses for these historic spreading episodes were estimated assuming that the average widening at all points along the rift is 1.8 cm/year. In addition, it is assumed that during a dike injection episode, no thicker dike can be injected than corresponds to the amount of potential extension accumulated since the last episode at that latitude, a reasonable assumption in the absence of any direct evidence for the thicknesses of the intruded dikes throughout the elastic layer. This implies that the dikes taper where they overlap one another along the strike of the rift zone. This has been approximated by square-ended dikes for modeling purposes. It is assumed that no unreported rifting events occurred since the 1618 Theistareykir episode, that 150 years prior to that episode

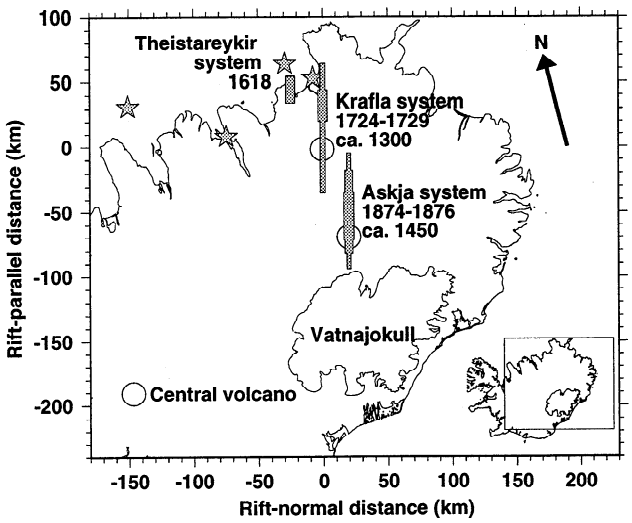

Figure 7. Map of northeast Iceland showing the date, location, and dimensions of previous rifting episodes in the NVZ, and recent, large earthquakes in the TFZ. The stars give the locations of the modeled events in the TFZ. The Krafla caldera is positioned at $x = y = 0$.

(the event recurrence time [*Björnsson*, 1985]), rifting occurred in the Askja system, and 150 years prior to that in the Krafla system. These assumptions enable estimates to be made for the dike thicknesses of historic episodes, throughout the elastic layer, and values similar to that known for the recent Krafla episode were obtained, a reasonable result. Dike lengths used were based on historical reports of the extent of surface fissuring [e.g., *Tryggvason*, 1984].

A value of 7 m was obtained for the thickness of the dike complex inferred to have been injected in the Theistareykir system in 1618. This value is probably an upper bound as the dike is thought to be fairly short (~20 km), and a thickness of 7 m yields an aspect ratio of 0.29 x 10^3 which is somewhat high for Icelandic dikes [*Gudmundsson*, 1984]. However, dikes as thick as 10 m are observed in this region [*Gudmundsson*, 1995b]. A similar maximum thickness was obtained for the 1724–1729 Mývatn Fires episode. A dike of variable along-strike thickness was used that tapers where it overlaps with the preceding 1618 Theistareykir dike. For modeling purposes, three end-to-end dikes, simultaneously intruded in 1729, were used to simulate the intrusion, a northern and a southern one with thicknesses of 4 m and a central one with a thickness of 7 m (Figure 7). For the 1874 Askja episode, a dike with a thickness of 8 m along much of its length was obtained. Five end-to-end, simultaneously injected dikes were used, with thicknesses of 3 m, 6 m, 8 m, 6 m, and 3 m, to simulate a single dike that tapers to the north and south (Figure 7).

Teleseismic focal mechanisms for large earthquakes in the TFZ show that they are predominantly right-lateral strike-slip [*Einarsson*, 1991]. All events large

enough, close enough, or recent enough to significantly affect points of the GPS network were modeled using a version of the elastic-viscoelastic modeling program adapted for strike-slip sources (T. T. Yu, personal communication, 1995). Estimates of the fault length and amount of slip for each event were made using the relations $M = 2/3 \log M_0 - 10.7$ [*Hanks and Kanamori*, 1979], where M is the magnitude and M_0 is the seismic moment (in dyne centimeters), and $M_0 = \mu A \bar{u}$ [e.g., *Aki and Richards*, 1980], where μ is the rigidity, A is the area of fault slip, and $\bar{u}$ is the amount of slip. In a strict sense the TFZ is segmented on a scale of ~25 km [*Einarsson*, 1991]. We assume for modeling purposes that magnitude ~6 and ~7 events rupture one and two segments respectively, and this suggests fault lengths of about 25 km and 50 km for these events. The estimate for the magnitude ~6 events is supported by the length of the aftershock zone of the 1976 M6.4 event [*Björnsson et al.*, 1977]. All events were assumed to rupture the whole elastic layer, and thus slip estimates of 2 m and 0.5 m were obtained for the magnitude ~7 and ~6 events.

Substantial, local, recent vertical motions are reported close to the Askja central volcano (see *Camitz et al.* [1995] for summary) that are consistent with pressure changes in a shallow magma chamber [*Tryggvason*, 1984]. On the basis of tilt measurements for 1988–1991, *Rymer and Tryggvason* [1993] concluded that 80% of the observed ground deformation could be explained by the deflation of a spherical magma chamber centered at 65°3.19'N, 16°46.10'W and at a depth of 2.8 km. Preliminary investigations of the probable effect of the recent Krafla rifting episode on vertical motion in the neighborhood of the Askja central volcano show that this cannot explain the observations. It can therefore be concluded that deflation of the magma chamber probably did occur and that this effect must be included in modeling the 1987–1992 deformation field. An average deflation of 4.8 cm/year was assumed [*Rymer and Tryggvason*, 1993], using a simple Mogi model of a point source in an elastic half-space [*Mogi*, 1958].

The total effect of all the historical and recent tectonic processes mentioned above is shown in Figures 8 and 9. The horizontal deformation field is complicated. Predicted displacements decrease with distance from the rift zones. The maximum displacement is 4 cm, occurs close to the Askja caldera, and is mostly a result of the deflation of the Askja magma chamber 1987–1992. Apart from this, the maximum displacements occur to the north of the Askja system and to the southwest of the Krafla system. A maximum motion of about 1.5 cm is expected there. The displacements shown are relative to the total model, and within this framework points east of the Askja system undergo little motion, as do points in the far south, west, and east of the network.

The vertical field shows that a maximum subsidence of 2.7 cm occurs in the vicinity of the Askja caldera (Figure 9) and uplift of 0.4 cm occurs in the Krafla volcanic system. The vertical motion resulting from the processes and episodes modeled is thus small.

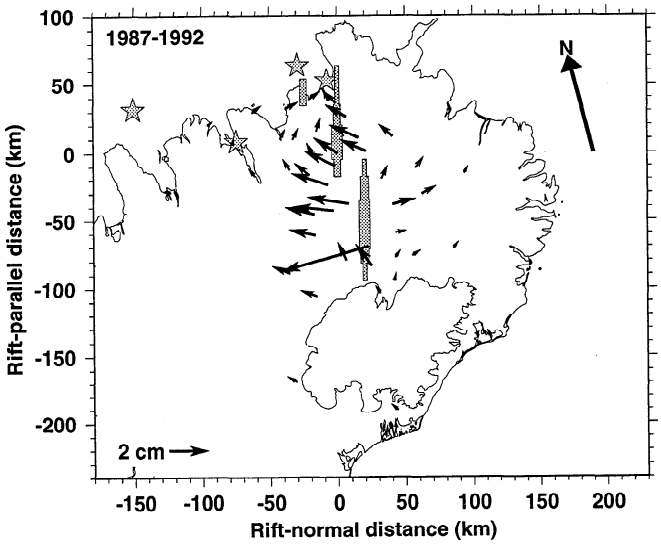

Figure 8. Total horizontal displacements for 1987–1992 of points of the GPS network as a result of historical episodes in the NVZ, recent, large earthquakes in the TFZ, and magma chamber deflation at the Askja volcano.

Krafla Rifting Episode

The effects of the historical episodes and earthquakes and deflations of the Askja magma chamber were subtracted from the observed horizontal and vertical deformation fields, and the residual fields modeled as viscoelastic relaxation following the 1975–1985 Krafla rifting episode. The final model resulted from trying a large number of forward models and selecting the best fit model that minimized, in a least squares sense, the differences between the predicted and observed displacements 1987–1992. Consistency was maintained with previous estimates for the dike thicknesses based on the measured amount of surface expansion within and across the fissure swarm and the amount of contraction outside of it [*Tryggvason*, 1984]. Dike lengths are based on reports of the extent of surface fissuring.

Four end-to-end dike segments, simultaneously injected in 1979 were used to simulate the along-strike variation in the thickness of the dike. This is a simple method of modeling a continuous dike of variable along-strike thickness, and we do not imply that four dikes were actually intruded. In reality, the dikes were injected over a period of about 9 years. Modeling the intrusions as such, however, surprisingly produces negligible differences in the resultant deformation field for 1987–1992 when compared with the simultaneously injected approximation. From south to north dike thicknesses of 4.5 m, 5.0 m, 4.5 m and 3.0 m were used. All other model parameters were identical to those given in Table 3. Figure 10 illustrates the fit of the model to the points in the profile zone (Figure 4).

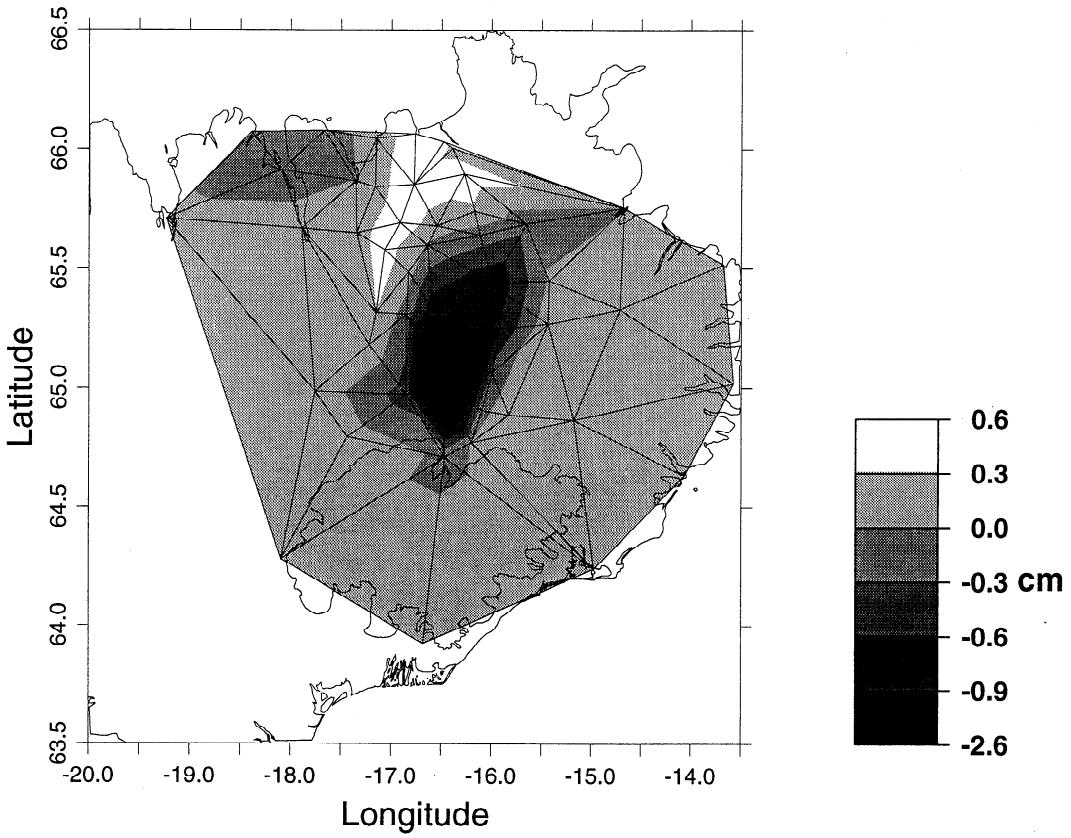

Figure 9. Total vertical displacements for 1987–1992 of points of the GPS network as a result of historical episodes in the NVZ, recent, large earthquakes in the TFZ, and magma chamber deflation at the Askja volcano. The vertical motions of the points, whose positions are at the corners of the triangles, are shown, along with bilincarly interpolated, contoured displacements between them. No observations exist between the points, and this illustrative method is adopted for clarity only. The scale bar gives vertical displacement in centimeters.

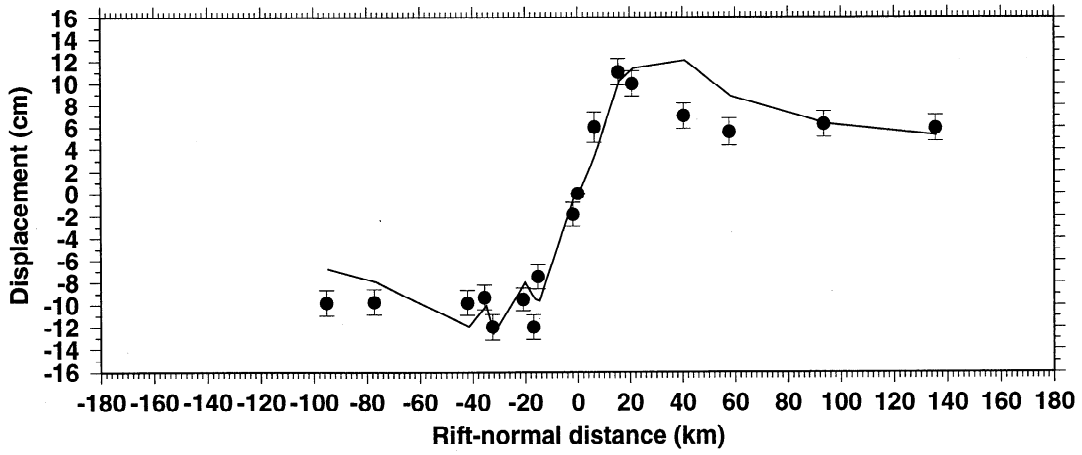

Figure 10. Comparison of observed and best fitting simulated horizontal displacements for 1987–1992 of points within the profile zone shown in Figure 4. The effects of the historical episodes in the NVZ, TFZ, and magma chamber deflation at the Askja volcano have been subtracted from the observed displacements.

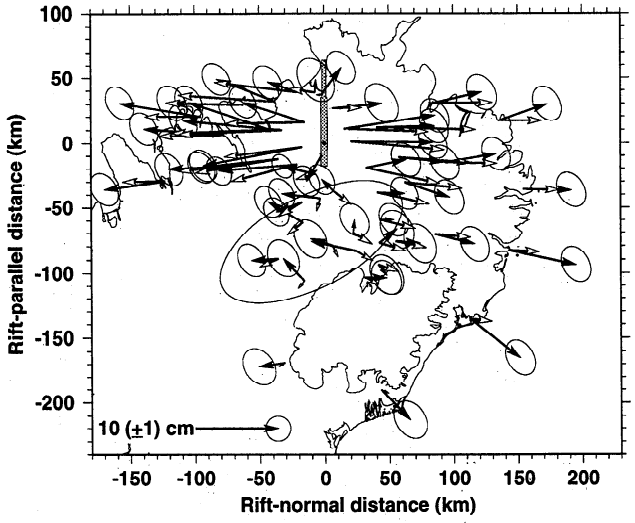

Figure 11. Comparison of observed and best fit simulated displacements for 1987–1992. The solid arrows represent the observed displacements minus the effects of the historical episodes in the NVZ, TFZ, and magma chamber deflation at Askja. The open and solid arrows indicate simulated displacements. The position of the dike and its dimensions are shown schematically.

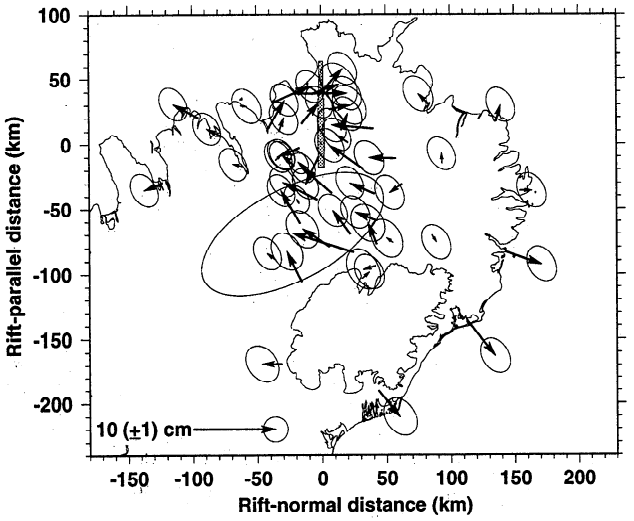

Figure 12. The residual displacement vectors remaining after subtracting the best fit simulated displacements from those observed in 1987–1992.

A maximum expansion of 24 cm is predicted for the period 1987–1992 (Figure 10), occurring at distances of ~40 km from the rift. Farther away, the expansion decreases to ~12 cm. The observed displacements are well modeled, although the observed maximum displacement occurs closer to the rift and has a somewhat shorter wavelength than is predicted. A reasonable fit to the farthest points is achieved, with motion underestimated by ~3 cm at distances of 100 km west of the rift. In plan view, the model predicts quasi-radial horizontal displacements outward from the dike at all points (Figure 11). Displacement directly to the south and north of the dike is considerably smaller than that on either side of it, and points in the far south of the network are predicted to have experienced 1–3 cm of motion 1987–1992.

The residual horizontal field is shown in Figure 12. There are two significant areas of misfit. The first is within the NVZ, where radial motion is overestimated by up to ~5 cm at a number of points. The second is in the far south and southeast of the network, where residuals of up to ~7 cm remain. No other areas of systematic residuals, significant at the 2σ level, are evident.

The model predicts relative uplift of up to ~11 cm close to the rift axis (Figure 13). The uplift decreases to zero at about 20–40 km from the dike. At greater distances the predicted relative uplift is ~4 cm at distances of ~100 km from the dike. Of the points in the profile zone, only four out of 17 do not fit the model to within 3σ, and all of these are within ~20 km of the dike axis. The observed and predicted two-dimensional vertical fields are shown in Figure 14. The model predicts the observations qualitatively, with uplift predicted above the dike relative to more distant areas, but in general, the observed amplitudes of vertical displacement are

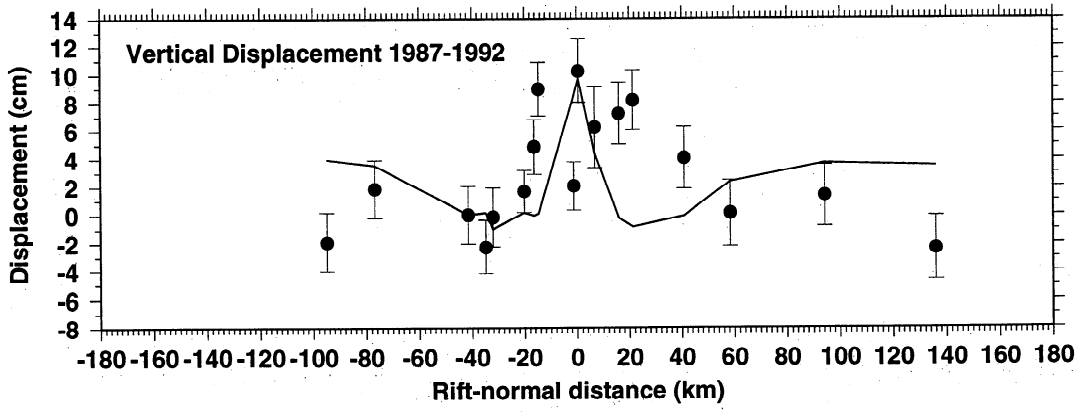

Figure 13. Same as Figure 10, except for the 1987–1992 vertical deformation field.

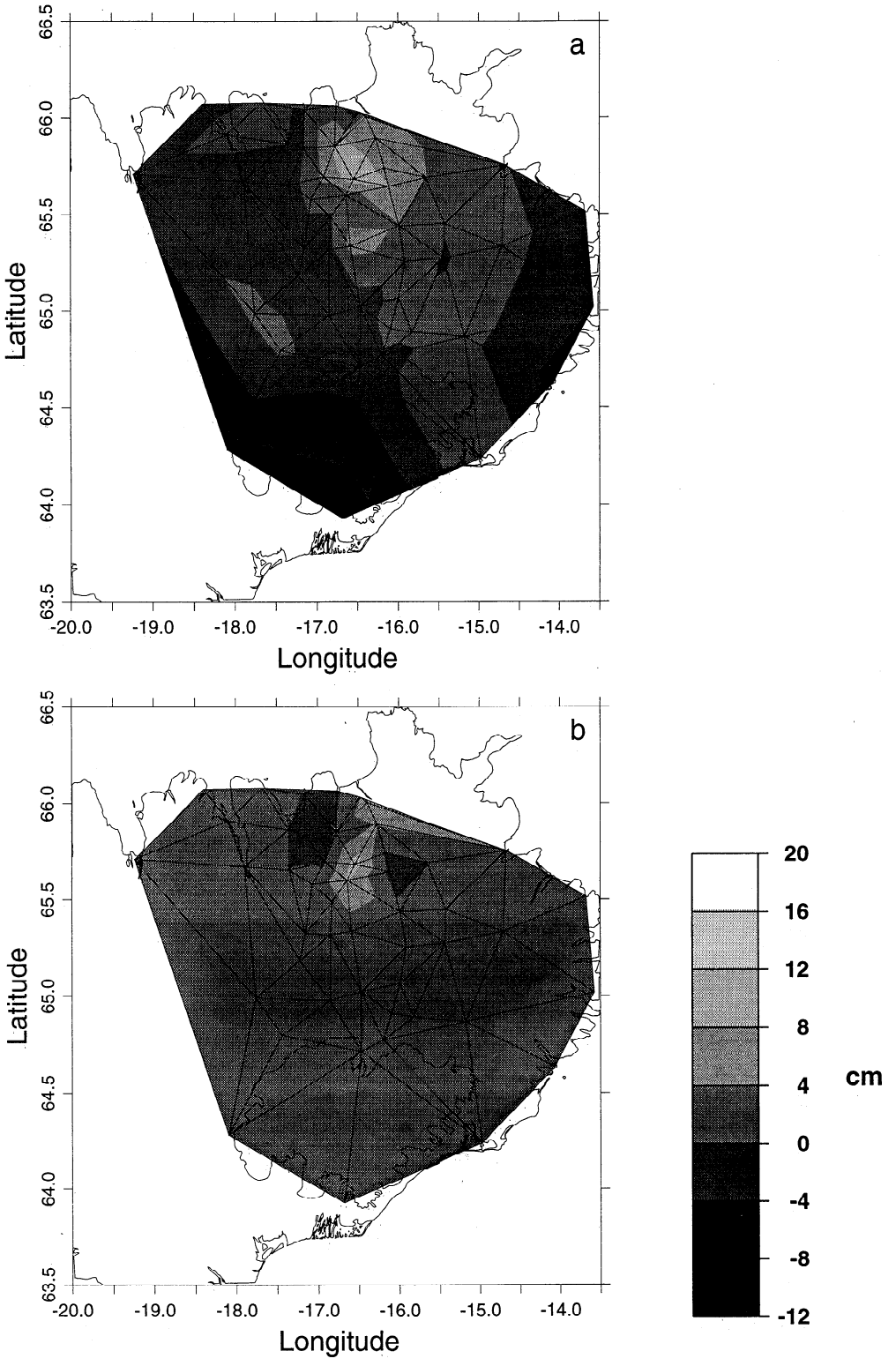

Figure 14. (a) Observed vertical displacements minus the effects of the historical episodes in the NVZ, TFZ, and magma chamber deflation at the Askja volcano, and (b) simulated motions for 1987–1992 resulting from the recent Krafla rifting episode, using the model that fits best the 1987–1992 horizontal field. Pictorial representation as for Figure 9.

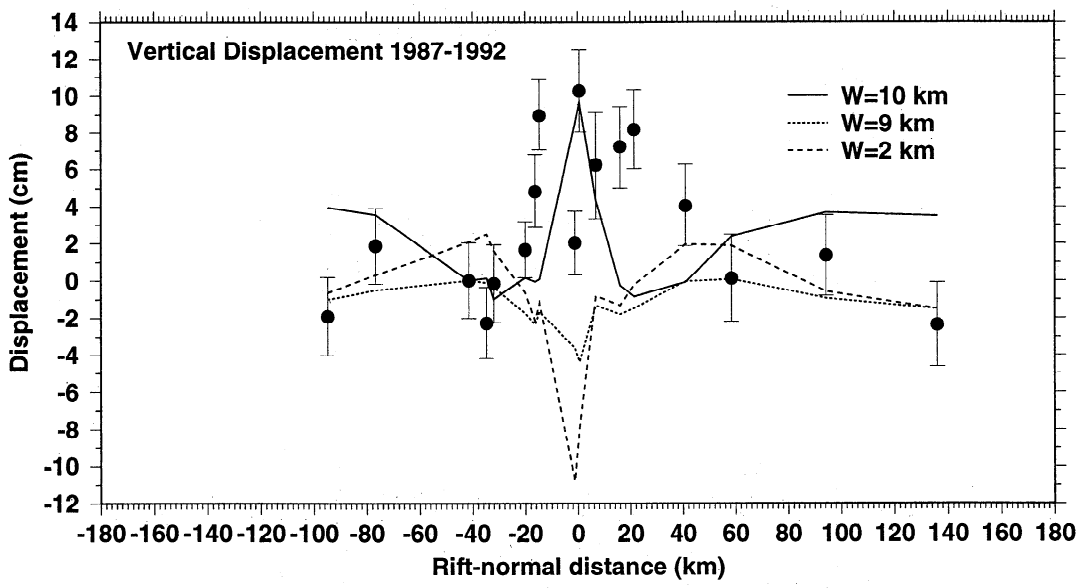

Figure 15. Comparison of observed and simulated vertical displacements for 1987–1992 of points within the profile zone shown in Figure 4 for dikes extending completely ($W = 10$ km) (solid curve) and partially ($W = 9$ km, $W = 2$ km) (short-dashed curves) through the elastic layer. All other model parameters are identical to those given in Table 3. The effects of historical episodes in the NVZ and TFZ, and magma chamber deflation at the Askja volcano have been subtracted from the observed displacements; 1σ error bars are shown.

less well modeled, particularly in the far south of of the network, where other processes may be at work.

Discussion

Quality of the Model

Modeling of the effects of earlier historical rifting episodes and earthquakes in North Iceland is subject to considerable uncertainty because of the scarcity of information about the event dimensions. Furthermore, the effects of these processes are small in comparison with that of the recent Krafla rifting episode. For this reason, incorporating these effects into the model made little difference, and it could, indeed, be argued that making such small and uncertain corrections merely increased the noise in the deformation field. Nevertheless, modeling these effects illustrates the style and timescales of deformation following typical large events in Iceland.

The layer densities were estimated from seismic velocities and a standard velocity-density relationship for Iceland [*Christensen and Wilkins*, 1982]. The variations in seismic velocity and the uncertainty in the velocity-density relationship indicate density variations and uncertainties of ~10% in both the elastic layer and viscoelastic half-space. Previous results using a dip-slip source indicate that varying the layer and half-space densities by 10–20% produces little difference in the predicted displacement fields [*Rundle*, 1981]. From this we conclude that the density variations expected in Iceland will have little effect on the modeling results.

Observed variations of v_p and the v_p/v_s ratio with depth indicate variations and uncertainties in the average elastic moduli of ~25%. Variations in μ_h are most likely to affect the modeling results since it is this parameter that has stress relaxation properties. Example calculations show that a variation of μ_h on this scale will not significantly change the amplitude of the displacement field (compare Figures 2 and 3 of *Hofton et al.* [1995]). Thus the expected variations in μ_h will not significantly affect the results of the present analysis.

The elastic layer thickness is conjectured to lie in the range ~8–12 km from magnetotelluric evidence for a low-resistivity layer at ~10 km depth beneath the NVZ and seismological evidence for the depth extent of earthquakes. Support for this may be found in considerations of the height of the dike. Estimates of the height of injected dikes based on the amount of surface widening and the volume of injected lava that flowed out of the Krafla magma chamber are ~2 km [*Björnsson*, 1985]. However, lava of differing chemical composition erupted northerly in the fissure swarm [*Björnsson*, 1985], and estimates of ~8.5 km for the depth of the dike bottom from geodetic data modeling [*Rubin*, 1992] provide evidence that the dike extends much deeper than 2 km, with the extra material required being injected from greater depths [*Björnsson*, 1985; *Gudmundsson*, 1995b]. In that case, the dike probably ruptured down as far as the partially molten material, i.e., down to a viscoelastic region. The height of the dike may thus indicate the thickness of the elastic layer.

Evidence for large dike heights is available for only some intrusive events, and it is possible that only some events ruptured the entire elastic layer. However, minor vertical subsidence is predicted above a dike that

does not rupture the entire elastic layer (Figure 15). The spatial extent of the deformation scales approximately by $1/H$, the inverse of the elastic layer thickness. An elastic layer thickness larger than 10 km would thus degrade the fit of the horizontal deformation field. The fit to the vertical deformation field would improve but only significantly if the elastic layer thickness were made several times greater, a value inconsistent with the other constraints available (see Figures 10 and 13). Furthermore, the amplitude of the predicted motions is heavily dependent on the depth extent of the dike, and the observations cannot be matched by dikes of heights substantially less than 10 km in vertical extent. These factors together provide compelling evidence that the dike ruptured to the bottom of the elastic layer and that both are ~10 km high.

Prior to 1980, deflation of the Krafla magma chamber was accompanied by injection of magma into the fissure swarm to form dikes, and very little lava was erupted. Inverse modeling of geodetic data collected 1975–1980 encompassing ~14 dike emplacement events indicated dikes in the depth range 1.25–8.5 km [*Rubin*, 1992]. Although surface fissuring accompanied all the events, this evidence suggests that the dikes did not all reach the surface.

The postrifting deformation data favor, however, a dike that extends to the surface, since a buried dike is predicted to produce contraction within ~5 km of the rift 1987–1992 [*Hofton*, 1995]. This conclusion is supported by the fact that after 1980 surface lava flows accompanied most of the dike injections and smaller amounts of rift widening were observed than in the earlier events [*Tryggvason*, 1984]. An explanation for the results of *Rubin* [1992] may thus be that some early, individual dikes of the complex did not reach the surface but that later dikes were proportionally wider at their tops than at their bottoms.

A total length of 82 km was assumed for the Krafla dike, consistent with the best estimate for the length of the activated fissure swarm of 80–90 km, as indicated by seismicity and opening of new ground fissures [*Tryggvason*, 1984]. Variations in dike length of about 10% do not significantly alter the predicted displacement fields and have most effect on the form of the deformation field near the ends of the dikes [*Hofton*, 1995].

Dike dips are observed in the field to vary by ~5° [*Gudmundsson*, 1995a]. The dominant effect of altering the dike dip by ±10° is to shift the predicted displacement profile up or down. The deformation data are thus insensitive to small dip changes, and no improvement in the fit is obtained compared to using the simplifying assumption of a vertical dike.

Dike thickness estimates for the Krafla spreading episode were summarized by *Tryggvason* [1984] and *Gudmundsson* [1995b]. Observations of the width of the dike in the region of the caldera show up to 9 m of widening along a 12-km length of the fissure swarm. Outside of this region, dike thickness estimates were based on observations of widening between points on either side of the fissure zone, crudely corrected for contraction between the fissures by assuming an average contraction of 200 mm/km, perpendicular to the strike of the fissure swarm, a figure determined from the amount of flank contraction measured on either side of the fissure swarm. Because of this approach, the estimates of *Tryggvason* [1984] may be considered to be upper bound thicknesses. "High" and "low" estimates were presented where constraints were poor (Table 4). The best fit dike thicknesses found from modeling the 1987–1992 deformation data are close to the "low" estimates of *Tryggvason* [1984] (Table 4) and less than the local observed dike thickness in the region of the caldera. The reason for this may be because the true dike thicknesses vary with depth; for example, an elliptical shape may more accurately reflect the true shape of the injected dike and the width of the dike may be near its maximum at the surface [*Gudmundsson*, 1990].

After accounting for all the major, known tectonic events in north Iceland, significant residual motion remains in both the horizontal and vertical displacement fields, in the vicinity of the dike, and in the far south of the network. Variations in the model parameters are not able to explain these residuals, and they are thus probably attributable to either other tectonic processes, unmodeled complexities, e.g., structural heterogeneity, or simplifying assumptions in the model, e.g., Maxwell viscoelasticity.

Candidate intrusions in the Grimsvötn volcano (Figure 1), the Askja and Kverkfjöll (Figure 1) volcanic systems, and the Öræfajökull–Snæfell flank zone (Figure 1) were modeled in an attempt to explain the residual horizontal field [*Hofton*, 1995]. None of these models was completely successful, and the latter two are unsupported by any observations of seismic or volcanic activity. Activity in the Öræfajökull–Snæfell zone can explain the orientations of the residual vectors, and 2 m of widening at a depth of 2–10 km in 1983 is sufficient to model the amplitude of the residuals. Deeper intrusions at this location would produce the required orientations, but then larger intrusion thicknesses would be required. Dike injection later than 1983 would reduce

Table 4. Estimates of Dike Thickness With Distance From the Krafla Caldera

Distance Along Fissure Swarm, km	Dike Thickness, m	
	Tryggvason [1984]	This Study
35 to 44	3–5	3
20 to 35	5–7	4.5
−5 to 20	7.5	5
−18 to −5	4.5	4.5

Negative distances indicate distances to the south of the caldera.

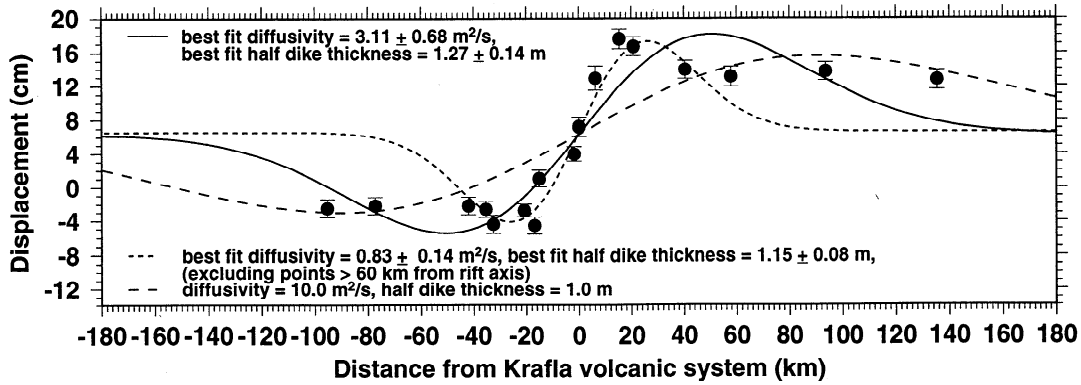

Figure 16. Horizontal displacements 1987 1992 as a function of distance from the spreading axis for the points within the profile zone shown in Figure 4. Vertical bars indicate 1σ errors. The best fit curves for models of stress diffusion in an elastic layer overlying a viscous layer are superimposed. A one-dimensional model (infinitely long dike) was used.

the required dike thickness. Such a model, however, predicts displacements of a comparable magnitude both southeast and north of Vatnajökull, but these latter are not observed.

The unexplained vertical motion observed around the ice cap Vatnajökull (Figure 1), fits very poorly a model of isostatic uplift centered on the present ice cap [*Sigmundsson*, 1991; *Sigmundsson and Einarsson*, 1992; *Hofton and Foulger*, this issue]. The vertical displacement field obtained from independent processing using the GEONAP software reveals a very similar pattern to that obtained using the Bernese results (Figure 14a) (C.-H. Jahn, personal communication, 1995), which suggests that the deformation is not an artifact of the data processing method.

Other Possible Models

Following the method of *Foulger et al.* [1992], a one-dimensional stress diffusion model was applied to the 1987–1992 displacements, which were viewed as instantaneous velocities 13 years after the dike intrusion event. The best fitting form (in a least squares sense) of the one-dimensional horizontal velocity equation [*Foulger et al.*, 1992, equation 4] to the observations was found and estimates of the dike thickness and stress diffusivity obtained. A best fit model to a profile perpendicular to the rift axis within the zone shown in Figure 4 yields an estimate for the half thickness of the dike (averaged throughout the elastic layer) of 1.27 m and a stress diffusivity of 3.11 m^2/s (Figure 16). It is clear from Figure 16 that there is a systematic misfit between the observations and the model. Increasing the diffusivity to 10 m^2/s (the value calculated by *Heki et al.* [1993] from two-dimensional modeling of the 1987–1990 deformation field) gives a better fit to points at large distances from the rift zone but at the expense of the fit to the points close to the rift. Excluding the points farther than 60 km from the rift yields a diffusivity of 0.83 m^2/s and fits the points close to the rift zone well but those far from the rift zone poorly. It is clear, in the light of the improved constraint on the deformation field provided by the 1992 survey, that the viscous stress diffusion model of *Foulger et al.* [1992] is insufficiently realistic to model the observations. The viscoelastic model presented here fits the observations much better.

An alternative, conceptually different explanation for the transient deformation field observed during 1987–1992 in north Iceland involves continuous, aseismic dike intrusion at depth beneath the Krafla spreading segment, a process which may be modeled using an elastic half-space (J. Savage, personal communication, 1994). Dike injection in an elastic half-space produces horizontal displacement fields that increase steeply to a peak within a few tens of kilometers from the spreading axis and then fall off more slowly at greater distances (Figure 17a) [*Foulger et al.*, 1994]. Zero vertical motion is predicted along the spreading axis, with substantial uplift on either side, peaking somewhat closer to the spreading axis than the horizontal motions, and decreasing with distance to zero farther away (Figure 17b).

Figure 17 shows the deformation resulting from two end-member dikes: a short, thick dike and a tall, thin dike. The model predicts the overall shape of the observed deformation field well and suggests that a range of dikes with various depths and dimensions intermediate to those shown will fit the observations. A statistically perfect fit using the continuous dike injection model would certainly be possible if a complex of dikes of various dimensions and times and rates of intrusion were used and probably a large suite of possible combinations would be allowable.

Proponents of the continuous dike injection model envisage the process as follows. At a spreading plate boundary, a large dike intrusion at shallow depth will produce increased extensional stress levels at its base, encouraging the upward leakage of magma and resulting in continued, postrifting dike injection and surface

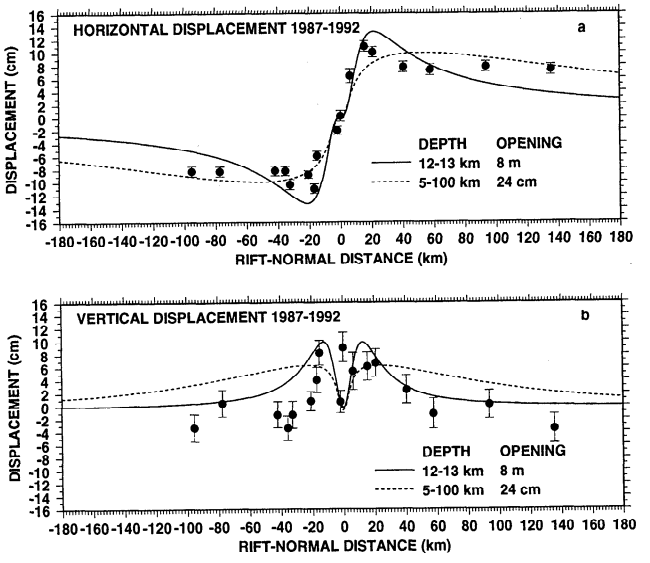

Figure 17. (a) Horizontal and (b) vertical displacements for 1987–1992 as a function of distance from the plate boundary for the points within the profile zone shown in Figure 4. Vertical bars indicate 1σ errors. Lines are theoretical curves for models of continuous dike intrusion at depth in an elastic half-space. The depth extent and amount of opening for the modeled dikes are given. Two end-member cases are shown, a short, thick dike and a tall, thin dike.

deformation in the same sense as the corifting deformation. The strike-slip and normal fault counterparts of this model have been widely applied to modeling regional motion around the San Andreas and other fault zones [e.g., *Williams*, 1995] and to modeling accelerated, postseismic deformation. At divergent plate boundaries this is to a large extent an ad hoc interpretative approach, yielding estimates of the dimensions of active zones and rates of motion that are not based on independent, supporting data and have limited ability to contribute to our understanding of the Earth or our predictive capabilities. The Earth at depth is known from isostatic uplift to flow over long time periods, and the very high temperature gradients and abundant, widespread volcanism in Iceland suggest that exceptionally low viscosity material occurs at relatively shallow depth. In view of this, and despite the fact that continuous dike injection models can be found that fit the data, models involving viscous flow are most appropriate in modeling deformation in Iceland.

In reality, dike injection throughout the elastic layer may not have been absolutely instantaneous during the Krafla rifting episode. Enormously increased stress levels at the lower tip of the dike after the injection are thought to have encouraged rapid, deep dike injection immediately afterward, extending the dikes to the base of the elastic layer. The timescale of this process is not known, as geodetic measurements at the required times are not available, and downward extension of the shallow dike may have taken weeks or months. A hybrid model involving both viscoelastic and continuous dike injection mechanisms is thus possible, but the deformation data are currently insufficient to determine whether such a process operates.

Viscosity Beneath Iceland

A summary of existing estimates for the viscosity beneath Iceland is given in Table 5. The first four were obtained from glacio-isostatic modeling [*Sigmundsson*, 1991; *Sigmundsson and Einarsson*, 1992], and from one- and two-dimensional elastic-viscous modeling of the deformation field in north Iceland [*Foulger et al.*, 1992; *Heki et al.*, 1993]. The range in these estimates is 0.3–50 x 10^{18} Pa s. The fifth is the value predicted by the present study and is included for comparison.

Spatial variations in viscosity are expected, for example, locally beneath Krafla and within and outside of the rift zone. Of the five estimates given in Table 5, the validity of the second study has been brought into question by the current deformation results [*Hofton and Foulger*, this issue] and the third and fourth are superseded by the fifth (this study). Of the two remaining estimates, from the first and fifth studies, one concerns southeast Iceland and a timescale of ~1000 years and the other northeast Iceland and a timescale of ~10 years. The estimate for northeast Iceland is an order of magnitude lower than that for southeast Iceland. Trade-offs between viscosity and other parameters, e.g., dike thickness, are possible within the framework of the model. Varying the dike thicknesses between the extreme values of *Tryggvason* [1984] was found to require viscosities in the range 1.0 ± 0.1 x 10^{18} Pa s. Radically different viscosities, for example, 90 x 10^{18} Pa s, fit poorly the displacements at large distances especially

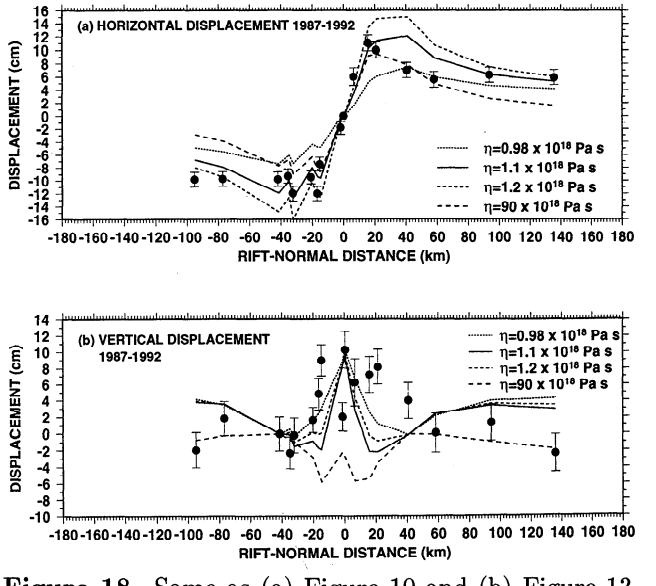

Figure 18. Same as (a) Figure 10 and (b) Figure 13, except for a suite of different viscosities.

Table 5. Estimates of Viscosity Beneath Iceland, Inferred From Geophysical Studies

No.	Viscosity Estimate, x 10^{18} Pa s	Reference	Source	Timescale, years
1	10	*Sigmundsson* [1991]	isostatic rebound	~1000
2	1–50	*Sigmundsson and Einarsson* [1992]	isostatic rebound	~100
3	0.3–2	*Foulger et al.* [1992]	stress redistribution	~10
4	3–20	*Heki et al.* [1993]	stress redistribution	~10
5	1.1	*Hofton and Foulger* [this issue]	stress redistribution	~10

in the vertical (Figure 18). The estimate for northeast Iceland is thus tightly constrained.

It is not apparent on tectonic grounds why the viscosities of these two regions should vary. The study area in northeast Iceland is centered on the spreading plate boundary. The western half of the ice cap Vatnajökull is also centered on the neovolcanic zone and lies very close to the center of the hotspot, which is thought to be at Kverkfjöll. If anything, the viscosity beneath Vatnajökull might thus be expected to be lower than beneath northeast Iceland. The difference may be a result of the 3 orders of magnitude difference in the timescales of the motions studied.

Asthenosphere viscosity estimates using data from postglacial rebound studies in Canada and Fennoscandia are in the range 10^{19}–10^{21} Pa s [e.g., *Peltier*, 1986; *Officer et al.*, 1988]. Evidence was also found for a zone of relatively low viscosity (4 x 10^{19} Pa s) in the upper asthenosphere [*Cathles*, 1975]. The viscosity predicted beneath Iceland is exceptionally low on a global scale and is probably a consequence of the Icelandic hotspot and the mid-ocean ridge [*Sigmundsson*, 1991]. Hot mantle material beneath Iceland would cause low viscosity, a property which may characterize all mid-ocean ridges and hotspots. The contributions of the hotspot and the ridge are not separable, but the two would be expected to reinforce one another. Hotspots and plate boundaries are probably major contributors to lateral viscosity variations in the Earth.

Simplifying Assumptions

Although a major improvement on the stress-diffusion model, which simulated a subsurface layer, the viscoelastic model has several limitations. Simplifying assumptions inherent in the model include an elastic layer with uniform thickness and an infinitely thick viscoelastic region with a simplified linear rheology. The elastic layer in Iceland probably thickens away from the spreading axis [e.g., *Björnsson*, 1985], and this is ignored in our simple model. A large volume of work exists indicating that actual Earth structure is elastically heterogeneous [e.g., *Meissner and Strehlau*, 1982], involving several layers with contrasting rheologies and lateral variations. In particular, the incorporation of a mid crustal ductile layer, a more realistic Earth structure, and one that is supported by magnetotelluric measurements in Iceland [*Björnsson*, 1985] may be an important improvement over half-space models.

Laboratory measurements show that rock rheology is represented better by a power law rather than a linear viscoelastic relationship [e.g., *Kirby*, 1983]. An important area for future research is to estimate the effects of this on the model results and to explore whether GPS measurements could permit a nonlinear rheology to be recognized.

Conclusions

1. The 1992 GPS survey results provided point coordinates accurate at the subcentimeter level in the horizontal and at the 2-cm level in the vertical. Differencing the results with those from the 1987 survey revealed a horizontal network expansion of up to 22 cm and relative vertical motions of up to ~20 cm.

2. Forward modeling the deformation as postrifting stress redistribution following the Krafla rifting episode in a structure comprising an elastic layer overlying a viscoelastic half-space yields a best fit viscosity of 1.1 x 10^{18} Pa s, a relaxation time of 1.7 years, and an elastic layer thickness of 10 km for northeast Iceland.

3. Major earthquakes and rifting episodes in Iceland result in long-term stress redistribution which may result in significant regional surface deformations for centuries afterward. Historical events must thus be taken into account when modeling deformation in Iceland.

4. The Krafla dike injection episode ruptured the entire elastic layer, with the lower part of the dike being fed from below, in accordance with the models of *Björnsson* [1985] and *Gudmundsson* [1995b]. Average estimated dike thicknesses are smaller than the maximum dike widths observed at the surface.

5. The data are not diagnostic of different geophysical models; for example, models involving continuous dike injection at depth, viscoelastic relaxation, or a combination of the two can be found that fit the observations. We favor a viscoelastic relaxation model as this is supported by independent observations and is thus most realistic for Iceland. Models involving simple viscous elements fit the data poorly, however, and can be ruled out.

Acknowledgments. The authors would like to thank G. Seeber, C.-H. Jahn, and C. Völksen for use of the GEO-

NAP data; J. B. Rundle for advice on viscoelastic modeling and help with the code; T. T. Yu for use of the strike-slip version of the viscoelastic program; and B. R. Julian, A. Rubin and J. Savage for useful comments. Much of the work was done using software written by K. Heki. Funding was provided by NERC grants GR9/834 and GR9/161, and DFG grant Se313/8-4. M.A.H. was supported by a NERC Ph.D. studentship. A. Gudmundsson, R. Bilham, and an Associate Editor provided valuable suggestions for the improvement of this paper.

References

Aki, K., and P. G. Richards, *Quantitative Seismology*, vol. 1, 557 pp., W. H. Freeman, New York, 1980.

Björnsson, A., Dynamics of crustal rifting in NE Iceland, *J. Geophys. Res., 90*, 10151–10162, 1985.

Björnsson, A., K. Sæmundsson, P. Einarsson, E. Tryggvason, and K. Grönvold, Current rifting episode in north Iceland, *Nature, 266*, 318–323, 1977.

Björnsson, A., G. Johnsen, S. Sigurdsson, and G. Thorbergsson, Rifting of the plate boundary in north Iceland 1975–1978, *J. Geophys. Res., 84*, 3029–3038, 1979.

Bott, M. H. P., and D. S. Dean, Stress diffusion from plate boundaries, *Nature, 243*, 339–341, 1973.

Camitz, J., F. Sigmundsson, G. Foulger, C.-H. Jahn, C. Völksen, and P. Einarsson, Plate boundary deformation and continuing deflation of the Askja volcano, north Iceland, determined with GPS, 1987–1993, *Bull. Volcanol., 57*, 136–145, 1995.

Cathles, L. M., *The Viscosity of the Earth's Mantle*, Princeton Univ. Press, Princeton, N. J., 1975.

Christensen, N. I., and R. H. Wilkins, Seismic properties, density and composition of the Icelandic crust near Reydarfjördur, *J. Geophys. Res., 87*, 6389–6395, 1982.

DeMets, C., R. G. Gorgon, D. F. Argus, and S. Stein, Effect of recent revisions to the magnetic reversal time scale on estimates of current plate motions, *Geophys. Res. Lett., 21*, 2191–2194, 1994.

Einarsson, P., Earthquakes and present-day tectonism in Iceland, *Tectonophysics., 189*, 261–279, 1991.

Elsasser, W. M., Convection and stress propagation in the upper mantle, in *The Application of Modern Physics to the Earth and Planetary Interiors*, edited by S. K. Runcorn, pp. 223–245, John Wiley, New York, 1969.

Foulger, G. R., A GPS geodetic survey of the Northern Volcanic Zone of Iceland 1987, *EOS Trans. AGU, 68*#1236, 1987.

Foulger, G. R., C.-H. Jahn, G. Seeber, P. Einarsson, B. R. Julian and K. Heki, Post-rifting stress relaxation at the divergent plate boundary in Northeast Iceland, *Nature, 358*, 488–490, 1992.

Foulger, G. R., et al., The Iceland 1986 GPS geodetic survey: tectonic goals and data processing, *Bull. Géod., 67*, 148–172, 1993.

Foulger, G. R., M. A. Hofton, B. R. Julian, C.,-H., Jahn, and K. Heki, Regional post-diking deformation in northeast Iceland: A third epoch of GPS measurements in 1992, in *Proceedings of the CRCM 1993, Kobe, December 6–11, 1993*, pp. 99–105, 1994.

Gebrande, H., H. Miller, and P. Einarsson, Seismic structure of Iceland along RRISP-profile I, *J. Geophys., 47*, 239–249, 1980.

Gudmundsson, A., Tectonic aspects of dykes in northwestern Iceland, *Jökull, 34*, 81–96, 1984.

Gudmundsson, A., Emplacement of dikes, sills and crustal magma chambers at divergent plate boundaries, *Tectonophysics., 176*, 257–275, 1990.

Gudmundsson, A., Infrastructure and mechanics of volcanic systems in Iceland, *J. Volcanol. Geotherm. Res., 64*, 1–22, 1995a.

Gudmundsson, A., The geometry and growth of dykes, in *Physics and Chemistry of Dykes*, edited by G. Baer and A. Heimann, pp. 23–44, A. A. Balkema, Rotterdam, Netherlands, 1995b.

Hanks, T. C., and H. Kanamori, A moment magnitude scale, *J. Geophys. Res., 84*, 2348–2350, 1979.

Heki, K., A network adjustment program for the Bernese Global Positioning System data analysis software, *Geod. Soc. Jpn., 38*, 309–312, 1992.

Heki, K., G. R. Foulger, B. R. Julian, and C. -H. Jahn, Plate dynamics near divergent plate boundaries: Geophysical implications of postrifting crustal deformation in NE Iceland, *J. Geophys. Res., 98*, 14,279–14,297, 1993.

Hofton, M. A., Anelastic surface deformation in Iceland detected using GPS, with special reference to isostatic rebound and the 1975-1985 Krafla rifting episode, Ph. D. thesis, 259 pp., Univ. of Durham, Durham, England, 1995.

Hofton, M. A., and G. R. Foulger, Postrifting anelastic deformation around the spreading plate boundary, north Iceland, 2, Implications of the model derived from the 1987–1992 deformation field, *J. Geophys. Res.*, this issue.

Hofton, M. A., J. B. Rundle, and G. R. Foulger, Horizontal surface deformation due to dike emplacement in an elastic-gravitational layer overlying a viscoelastic-gravitational half-space, *J. Geophys. Res., 100*, 6328-6339, 1995.

Jahn, C.-H., A highly precise GPS-epoch measurement in the northeast volcanic zone of Iceland, in *Cahiers du Centre Européen de Géodynamique et de Séismologie*, pp. 292–304, edited by P. Paquet, J. Flick, and B. Ducarme, Cent. Eur. de Géodyn. et de Seismol., Luxembourg, 1990.

Jahn, C.-H., G. Seeber, G. R. Foulger, and P. Einarsson, GPS epoch measurements spanning the mid-Atlantic plate boundary in northern Iceland 1987–1990, in *Gravimetry and Space Techniques Applied to Geodynamics and Ocean Dynamics, Geophys. Monogr. Ser.*, vol. 82, edited by B. E. Schutz et al., pp. 109–123, AGU, Washington, D. C., 1994.

Kirby, S. H., Rheology of the lithosphere, *Rev. Geophys., 21*, 1458–1487, 1983.

Lee, E. H., Stress analysis in viscoelastic bodies, *Appl. Math., 13*, 183–190, 1955.

Meissner, R., and J. Strehlau, Limits of stresses in continental crusts and their relations to the depth-frequency distribution of shallow earthquakes, *Tectonics, 1*, 73–89, 1982.

Mogi, K., Relations between the eruptions of various volcanoes and the deformation of the ground surfaces around them, *Bull. Earthquake Res. Inst.Univ. Tokyo, 36*, 99–134, 1958.

Officer, C. B., W. S. Newman, J. M. Sullivan, and D. R. Lynch, Glacial isostatic adjustment and mantle viscosity, *J. Geophys. Res., 93*, 6397–6409, 1988.

Okada, Y., Surface deformation due to shear and tensile faults in a half-space, *Bull. Seismol. Soc. Am., 75*, 1135–1154, 1985.

Peltier, W. R., Deglaciation-induced vertical motion of the north American continent and transient lower mantle rheology, *J. Geophys. Res., 91*, 9099–9123, 1986.

Rothacher, M., G. Beutler, W. Gurtner, T. Schildknecht, and U. Wild, Documentation for Bernese GPS software version 3.2, Univ. of Bern, Bern, Switzerland, 1990.

Rubin, A., M., Dike-induced faulting and graben subsidence in volcanic rift zones, *J. Geophys. Res., 97*, 1839–1858, 1992.

Rundle, J. B., Viscoelastic crustal deformation by finite quasi-static sources, *J. Geophys. Res., 83*, 5937–5945, 1978.

Rundle, J. B., Static elastic-gravitational deformation of a layered half space by point couple sources, *J. Geophys. Res., 85*, 5354–5363, 1980.

Rundle, J. B., Vertical displacements from a rectangular fault in layered elastic-gravitational media, *J. Phys. Earth, 29*, 173–186, 1981.

Rymer, H., and E. Tryggvason, Gravity and elevation changes at Askja, Iceland, *Bull. Volcanol., 55*, 362–371, 1993.

Sigmundsson, F., Post-glacial rebound and asthenosphere viscosity in Iceland, *Geophys. Res. Lett., 18*, 1131–1134, 1991.

Sigmundsson, F., and P. Einarsson, Glacio-isostatic crustal movements caused by historical volume change of the Vatnajökull icecap, Iceland, *Geophys. Res. Lett., 19*, 2123–2126, 1992.

Tryggvason, E., Widening of the Krafla fissure swarm during the 1975–1985 volcano-tectonic episode, *Bull. Volcanol., 47*, 47–69, 1984.

Williams, S. D. P., Current motion on faults of the San Andreas system in central California inferred from recent GPS and terrestrial survey measurements, Ph. D. thesis, University of Durham, Durham, England, 1995.

Wübbena, G., The GPS adjustment software package–GEONAP–concepts and models, in Proceedings of the fifth International Geodetic Symposium on Satellite Positioning, pp. 452–461, Las Cruces, N. M., 1989.

G. R. Foulger, Department of Geological Sciences, University of Durham, South Road, Durham, DH1 3LE, England.

M. A. Hofton, IGPP/UCSD, Dept. 0225, 9500 Gilman Drive, La Jolla, CA 92093. (e-mail: mhofton@ucsd.edu)

(Received November 1, 1995; revised May 1, 1996; accepted July 29, 1996.)